Study of τ Decays to Four-Hadron Final States with Kaons

K.K. Gan[a*]

[a]Department of Physics, The Ohio State University, Columbus, OH 43210, USA

The rare τ lepton decays to four explicitly identified hadrons have been studied with the CLEO detector at the Cornell Electron Storage Ring (CESR) using $(7.56 \pm 0.15)\ fb^{-1}$ of data collected near $\sqrt{s} = 10.58$ GeV. The first statistically significant measurements of $\mathcal{B}(\tau^- \to K^-\pi^+\pi^-\pi^0\nu_\tau, \text{excluding } K^0) = (7.4 \pm 0.8 \pm 1.1) \times 10^{-4}$ and $\mathcal{B}(\tau^- \to K^-K^+\pi^-\pi^0\nu_\tau) = (5.5 \pm 1.4 \pm 1.2) \times 10^{-5}$ are presented, including the first observation of the decay $\tau^- \to K^-\omega\nu_\tau$ with branching fraction, $(4.1 \pm 0.6 \pm 0.7) \times 10^{-4}$. We also publish the first upper limit for $\mathcal{B}(\tau^- \to K^-K^+K^-\pi^0\nu_\tau) < 4.8\ (6.1) \times 10^{-6}$ at 90% (95%) confidence level (C.L.). We also measure for the first time the invariant mass distributions of the decays.

The suppressed decays of the τ lepton to final states with kaons provide a powerful probe of the strange sector of the weak charged current. Measurement of the branching fractions and invariant mass distributions of various strange final states are needed to extract the Standard Model parameters, the strange quark mass m_s and the Cabibbo-Kobayashi-Maskawa element V_{us}, from τ lepton decays with precision competitive with both K_{e3} decay and lattice determinations [1]. These high mass decays can also be used to improve constraints on the τ neutrino mass. In this paper, we present the first statistically significant measurements of the branching fractions for the decays $\tau^- \to K^-\pi^+\pi^-\pi^0\nu_\tau$(ex. K^0) [2] and $K^-K^+\pi^-\pi^0\nu_\tau$, as well as the first published upper limit for the decay $\tau^- \to K^-K^+K^-\pi^0\nu_\tau$. We also investigate the substructure of the decays $\tau^- \to K^-\pi^+\pi^-\pi^0\nu_\tau$ and $K^-K^+\pi^-\pi^0\nu_\tau$, yielding the first observation and measurement of $\tau^- \to K^-\omega\nu_\tau$. We also present the first measurements of the invariant mass distributions of the decays. Previous measurements of the decays $\tau^- \to K^-\pi^+\pi^-\pi^0\nu_\tau$ and $K^-K^+\pi^-\pi^0\nu_\tau$ [3,4] had very large statistical errors due to large τ migration backgrounds (non-signal τ events) as a consequence of limited particle identification capability. We also compare the branching fraction for the decay $\tau^- \to K^-\omega\nu_\tau$ to the prediction of Li [5] and find significant disagreement.

The data used in this analysis were collected with the CLEO III detector [6] at CESR near the center-of-mass energy 10.58 GeV. The sample corresponds to an integrated luminosity of $(7.56 \pm 0.15)\ fb^{-1}$ containing $(6.90 \pm 0.14) \times 10^6$ τ-pair events produced in e^+e^- collisions. The detector features a four-layer silicon strip vertex detector, a wire drift chamber, and a Ring Imaging Cherenkov (RICH) detector that is critical for this analysis. The specific ionization loss (dE/dx) measured in the drift chamber is used to identify hadron species with a resolution of about 6%. The RICH detector [7,8] surrounds the drift chamber and uses thin LiF radiators to generate Cherenkov photons from the incident charged particles. Generated photons propagate through an expansion volume of gaseous nitrogen at atmospheric pressure, and are detected by multiwire proportional chambers filled with a mixture of TEA and CH_4 gases. RICH particle identification (ID) is available within $|\cos\theta| < 0.83$, where the polar angle, θ, is with respect to the incident beam. The electromagnetic calorimeter surrounds the RICH detector and measures the energy, position, and lateral shape of showers induced by charged and neutral particles. The calorimeter contains 7784 CsI(Tl) crystals arranged in a barrel section ($|\cos\theta| < 0.83$) and two endcaps ($0.83 < |\cos\theta| < 0.95$). These com-

*Representing the CLEO III Collaboration. This work was supported by the National Science Foundation and the U.S. Department of Energy.

ponents operate inside a 1.5 T solenoidal magnetic field. A muon detection system surrounds the solenoid with iron absorber interspersed with wire chambers operated in proportional mode.

The $\tau^+\tau^-$ candidate events must contain four well-reconstructed charged tracks with zero net charge. Each event is divided into two hemispheres (tag and signal) using the plane perpendicular to the thrust axis [9]. The thrust axis is determined using all charged tracks and photons. We select events in a 1-vs-3 topology by requiring one and three tracks in the tag and signal hemispheres, respectively.

We require the missing momentum of the event to be in the central region of the detector ($|\cos\theta_{miss}| < 0.85$) to suppress radiative Bhabha and μ-pair backgrounds. In order to diminish hadronic background (e^+e^- annihilation events to quark-antiquark pairs) while maintaining a high acceptance for τ decays, we require the tag hemisphere to have invariant mass less than 1.2 GeV/c^2, and that of the signal hemisphere to be less than the τ lepton mass. Hemisphere masses are calculated using all photons and charged tracks. Charged tracks in the signal hemisphere are assigned masses according to particle ID, while tracks in the tag hemisphere are assigned the pion mass. In order to suppress two-photon backgrounds, we require that the total event visible energy be greater than 40% of the center-of-mass energy.

The momentum of tracks in the tag hemispehere must be greater than 100 MeV/c and must point into the central region of the detector, $|\cos\theta| < 0.90$. Charged pion and kaon track candidates in the signal hemisphere must have momentum greater than 200 MeV/c and satisfy $|\cos\theta| < 0.8$ for improved particle ID performance. To reduce beam-gas and τ-migration events with K^0_S, the distance of closest approach of each track to the e^+e^- interaction point (IP) must be within 5 mm transverse to the beam and 5 cm along the beam direction. To further reduce K^0_S background, we reject events containing a pair of tracks with detached vertex greater than 1 cm from the IP and $\pi^-\pi^+$ mass consistent with the nominal K^0_S mass. In order to reduce migration from events with photon conversion in the detector media as well as Dalitz decays of π^0, we reject an event if any track in the signal hemisphere is identified as an electron (see below).

Photon candidates are defined as isolated energy clusters in the calorimeter with a photon-like lateral shower profile and energy deposition greater than 60 (100) MeV in the barrel (endcap) region of the detector. Candidate π^0's are reconstructed from two-photon combinations using only photons in the barrel section of the calorimeter. For the $\tau^- \to K^-\omega\nu_\tau$ decay channel, a π^0 candidate must satisfy $-4.0 < S_{\gamma\gamma} < +3.0$, where $S_{\gamma\gamma} = (M_{\gamma\gamma} - M_{\pi^0})/\sigma_{\gamma\gamma}$ ($\sigma_{\gamma\gamma}$ is the mass resolution calculated from the energy and angular resolution of each photon pair in the event).

We do not explicitly veto events based on the photon multiplicity, thus allowing multiple π^0 candidates in an event in order to reduce the dependence on Monte Carlo simulation of fake photons. However, we reject an event if any photon in the hemisphere not used in π^0 reconstruction has energy in excess of 200 MeV, reducing feeddown from τ decays with more than one π^0 in the final state. To reduce combinatoric background, we also require the angle of the π^0 candidate momentum in the τ center of mass frame relative to the τ momentum in the laboratory frame satisfy $\cos\theta_{CM} > -0.75$. To boost a π^0 candidate to the τ rest frame, we approximate the τ energy as the beam energy, and the τ direction as along the visible momentum. Fake π^0's show an enhancement at $\cos\theta_{CM} \simeq -1$, as opposed to a depletion for the signal. In order to improve the ω mass resolution, the π^0 candidate is constrained to the nominal π^0 mass in calculating $M(\pi^+\pi^-\pi^0)$.

We combine information from specific ionization loss (dE/dx) and from the RICH system to determine whether a track is identified as a pion or kaon. The RICH detector response is distilled into a χ^2_i variable for each particle hypothesis ($i = \pi, K$). The value of χ^2_i is derived from the number of detected Cherenkov photons and their locations relative to the Cherenkov cone expected for a particle with given momentum and mass. The χ^2_i from the RICH are combined with σ_i, the number of standard deviation of the measured dE/dx from expectation for the particle hypotheses, into the variable $\Delta\chi^2 = \chi^2_\pi - \chi^2_K + \sigma^2_\pi - \sigma^2_K$.

A track is identified as a pion (kaon) if it satisfies $\Delta\chi^2 < 0$ (> 10). The more stringent kaon requirement is necessary to reduce migration from the dominant Cabibbo-favored τ decays with pions faking kaons. Efficiencies and fake rates in the Monte Carlo simulation are calibrated using kinematically selected $D^{*+} \to D^0\pi^+$ decays with $D^0 \to K^-\pi^+$ in the data [10]. The momentum-dependent particle identification efficiencies and fake rates are shown in Figure 1. The momentum-averaged kaon tagging efficiency is ∼89%, while the pion misidentification rate is ∼1%. For candidate $\tau^- \to K^-\omega\nu_\tau$ decays, we only identify the bachelor track and assume the tracks used to construct ω candidates are pions. For $\tau^- \to K^-\pi^+\pi^-\pi^0\nu_\tau$ (ex. ω) decays, we reject events with $M(\pi^+\pi^-\pi^0)$ within 30 MeV/c^2 of the nominal ω mass.

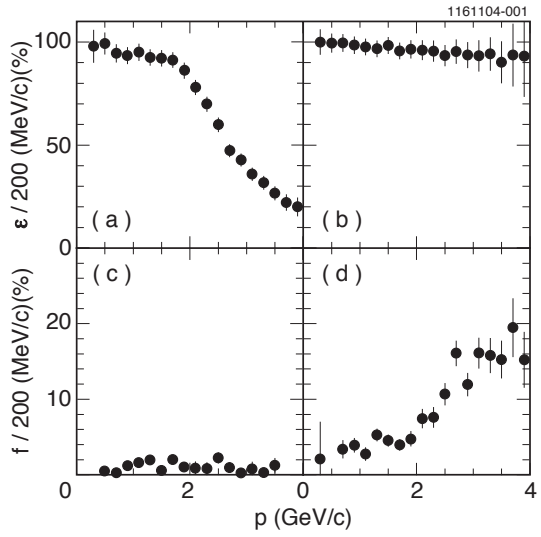

Figure 1. Momemtum-dependent particle identification efficiencies for kaons (a) and pions (b), and fake rates for π-as-K (c) and K-as-π (d). Error bars are statistical only.

The number of events in the decays $\tau^- \to K^-\pi^+\pi^-\pi^0\nu_\tau$ (ex. ω) and $K^-K^+\pi^-\pi^0\nu_\tau$ are extracted by fitting the $S_{\gamma\gamma}$ distribution using a Gaussian with a long low-mass tail over a polynomial background, in which the shape of the π^0 signal is constrained to the signal Monte Carlo expectation. For the decay $\tau^- \to K^-K^+K^-\pi^0\nu_\tau$, we simply require $-4.0 < S_{\gamma\gamma} < +3.0$; no events are observed in this window. The yield for $\tau^- \to K^-\omega\nu_\tau$ is extracted by fitting the $M(\pi^+\pi^-\pi^0)$ distribution using a Breit-Wigner lineshape [11] convoluted with a Gaussian resolution function over a polynomial background.

Hadronic backgrounds are calculated empirically using a sample of high-mass tagged events assuming the two jets fragment independently. The hadronic background calculation has been verified by finding consistent branching fraction measurements using a lepton (e or μ) tagged sample in which hadronic backgrounds are greatly suppressed. An electron candidate must have specific ionization loss consistent with that expected for an electron and the ratio of shower energy to momentum, $0.85 < E_{sh}/p < 1.1$. A muon candidate must penetrate at least three (five) absorption lengths of iron for track momentum less (greater) than 2.0 GeV/c.

Efficiencies and τ-migration backgrounds are estimated using Monte Carlo events generated from the `KORALB-TAUOLA` program [12] with the detector response simulated by the `GEANT` program [13]. We model the decay $\tau^- \to K^-\pi^+\pi^-\pi^0\nu_\tau$ (ex. ω) with the $K^-a_1^0$ intermediate state and the decays $\tau^- \to K^-K^+\pi^-\pi^0\nu_\tau$ and $K^-K^+K^-\pi^0\nu_\tau$ via phase space. The decay $\tau^- \to K^-\omega\nu_\tau$ is modelled with an equal mixture of $K_1(1270)$ and $K_1(1400)$ resonances. The signal, background, and detection efficiencies are summarized in Table 1. The largest sources of τ-migration backgrounds are from channels with a charged pion misidentified as a kaon.

We have investigated the hadronic mass spectra to search for substructure. Figure 2(a, c, e) shows the $h^-h^+h^-\pi^0$ invariant mass spectra for $\tau^- \to K^-\pi^+\pi^-\pi^0\nu_\tau$ (ex. ω), $K^-\omega\nu_\tau$, and $K^-K^+\pi^-\pi^0\nu_\tau$ events. The background- and efficiency-corrected spectra are shown in Figure 2(b, d, f). The two- and three-hadron substructure for $\tau^- \to K^-\pi^+\pi^-\pi^0\nu_\tau$ (ex. ω) decays are shown in Figure 3. There is no evi-

Table 1
Yields, backgrounds, efficiencies, and branching fraction measurements. The branching fraction for $\tau^- \to K^-\pi^+\pi^-\pi^0\nu_\tau$ excludes the K^0 and ω intermediate reasonances. The branching fraction for $\tau^- \to K^-K^+K^-\pi^0\nu_\tau$ corresponds to the 90% (95%) C.L. upper limit [15]. All errors are statistical except the second errors, when present, which are systematic.

Channel	yield	τ mig.	$q\bar{q}$ bg	ϵ (%)	$\mathcal{B}$ ($\times 10^{-4}$)
$K^-\pi^+\pi^-\pi^0$	833 ± 36	434 ± 14	153 ± 25	5.68 ± 0.17	$3.7 \pm 0.5 \pm 0.8$
$K^-\omega$	500 ± 35	194 ± 12	64 ± 20	5.61 ± 0.09	$4.1 \pm 0.6 \pm 0.7$
$K^-K^+\pi^-\pi^0$	48 ± 9	1 ± 1	9 ± 7	5.89 ± 0.12	$0.55 \pm 0.14 \pm 0.12$
$K^-K^+K^-\pi^0$	0	0	0	4.36 ± 0.10	$<$ 0.048 (0.061)

dence for K_1, ρ^0, or K^*. The $M(\pi^+\pi^0)$ spectrum (Figure 3(e)) indicates the presence of ρ^+ consistent with the $K^-a_1^0$ model expectation ($\chi^2/d.o.f. = 23/(17-1)$, C.L. = 11.2%); the observed $M(\pi^-\pi^0)$ spectrum (Figure 3(f)) is not inconsistent with the $K^-a_1^0$ model, $\chi^2/d.o.f. = 24/(13-1)$ (C.L. = 2.3%), though there is no clear indication of a ρ^-. The distribution of $M(\pi^+\pi^-\pi^0)$ in Figure 4 clearly shows an ω signal, as well as a small η meson peak consistent with expectations for the decay $\tau^- \to K^-\eta\nu_\tau$ [16,17]. This is the first observation of the decay $\tau^- \to K^-\omega\nu_\tau$. The Monte Carlo model with an equal mixture of $K_1(1270)$ and $K_1(1400)$ resonances describe the $K^-\omega$ mass distribution well, though we do not attempt to extract the relative fraction of the two K_1 intermediate states. There is no indication of K^* or ρ resonances in the decay $\tau^- \to K^-K^+\pi^-\pi^0\nu_\tau$.

Most sources of systematic uncertainty affect these channels similarly. These include the uncertainty in integrated luminosity (2%), τ-pair cross-section (1%), charged track reconstruction (0.5% per track), 1-prong tag branching fraction (0.1%), electron veto (1.5%), photon veto (3%), π^0 detection (8.8%), particle ID efficiency (1.1–3.0%), τ-migration background due to particle misidentification (8.1–15.6%) and limited Monte Carlo statistics (2.6–5.7%), hadronic background estimate (8.3–18.4%), and detection efficiency (1.7–3.0%) due to limited Monte Carlo statistics. The π^0 detection efficiency has been calibrated using the high statistics decay $\tau^- \to h^-\pi^0\nu_\tau$. The $\tau^- \to K^-\omega\nu_\tau$ channel has additional uncertainty due to the branching fraction of $\omega \to \pi^+\pi^-\pi^0$ (0.8%), model dependence from use of either K_1 model alone (2.6%), and from variation of the polynomial background parameterization in fitting the ω signal (2.5%). The branching fractions with systematic errors are summarized in Table 1.

In summary. we present the first statistically significant measurements of the branching fractions for $\tau^- \to K^-\pi^+\pi^-\pi^0\nu_\tau$ (ex. K^0) and $K^-K^+\pi^-\pi^0\nu_\tau$. The decay $\tau^- \to K^-\omega\nu_\tau$ has also been observed for the first time. The branching fraction is nearly a factor of two smaller than Li's prediction [5], $\mathcal{B}(\tau^- \to K^-\omega\nu_\tau) = \mathcal{B}(\tau^- \to K^-\rho^0\nu_\tau) = 7.5 \times 10^{-4}$, using a vector meson dominance model as well as $SU(3)_f$ relations between ρ and ω mesons. Comparing the measurement with the previous measurement of $\tau^- \to K^-\rho^0\nu_\tau$ [18], the ratio of branching fractions, $\frac{\mathcal{B}(\tau^- \to K^-\omega\nu_\tau)}{\mathcal{B}(\tau^- \to K^-\rho^0\nu_\tau)} = 0.26 \pm 0.11$, is likewise significantly lower than Li's prediction of 1 [19]. The branching fractions, $\mathcal{B}(\tau^- \to K^-\pi^+\pi^-\pi^0\nu_\tau$, ex. K^0, $\omega)$ and $\mathcal{B}(\tau^- \to K^-\omega\nu_\tau) \times \mathcal{B}(\omega \to \pi^+\pi^-\pi^0)$, can be combined to yield $\mathcal{B}(\tau^- \to K^-\pi^+\pi^-\pi^0\nu_\tau$, ex. $K^0) = (7.4 \pm 0.8 \pm 1.1) \times 10^{-4}$ [20], which is significantly more precise than previous measurements [3,4]. The measurement of $\mathcal{B}(\tau^- \to K^-K^+\pi^-\pi^0\nu_\tau)$ is almost an order of magnitude smaller than previous results [3,4] which were based on samples with significantly larger τ migration backgrounds due to limited particle identification capability. The result for $\tau^- \to K^-K^+K^-\pi^0\nu_\tau$ corresponds to the

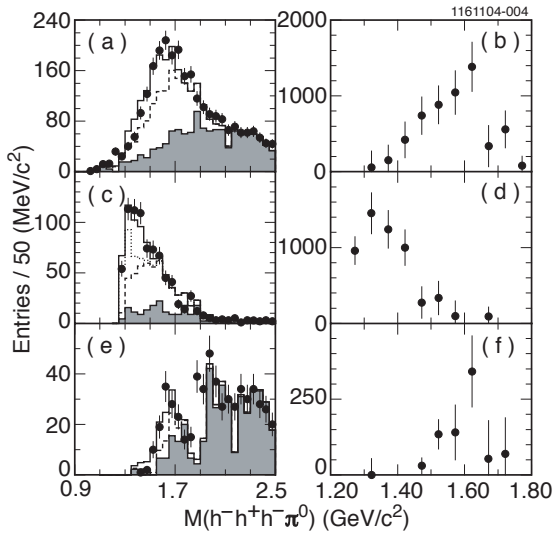

Figure 2. Four-hadron invariant mass spectra for $\tau^- \to K^-\pi^+\pi^-\pi^0\nu_\tau$ (ex. ω) (a), $K^-\omega\nu_\tau$ (c), and $K^-K^+\pi^-\pi^0\nu_\tau$ (e) events. The histograms show the expectations, including τ-migration Monte Carlo (dashed) and hadronic (shaded) background events. The dotted histogram in (c) shows the contribution of $K_1(1270)$. The distributions in (b, d, f) show the corresponding background- and efficiency-corrected spectra. Error bars are statistical only; (b, d, f) include errors in backgrounds and efficiencies.

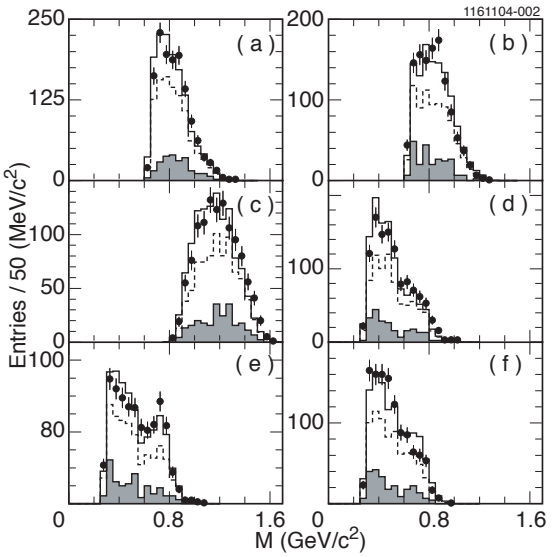

Figure 3. Two- and three-hadron invariant mass spectra (a) $K^-\pi^+$, (b)$K^-\pi^0$, (c) $K^-\pi^+\pi^-$, (d) $\pi^-\pi^+$, (e) $\pi^+\pi^0$, and (f) $\pi^-\pi^0$, in non-ω resonant $\tau^- \to K^-\pi^+\pi^-\pi^0\nu_\tau$ events. The histograms show the expectation including τ-migration Monte Carlo events (dashed) and hadronic background (shaded). Error bars are statistical only.

first published upper limit on this decay. These new results, together with the first measurements of the invariant mass distributions, provide important ingredients which can be used to extract the Standard Model parameters, m_s and V_{us}.

REFERENCES

1. E. Gamiz et al., Phys. Rev. Lett. 94 (2005) 011803.
2. Charge conjugate states are implied throughout this paper.
3. S.J. Richichi et al., CLEO Collaboration, Phys. Rev. D 60 (1999) 112002.
4. R. Barate et al., ALEPH Collaboration, Eur. Phys. J. C 1 (1998) 65.
5. Bing An Li, Phys. Rev. D 55 (1997) 1436; The ratio $\frac{\mathcal{B}(\tau^-\to K^-\omega\nu_\tau)}{\mathcal{B}(\tau^-\to K^-\rho^0\nu_\tau)}$ should be 1 instead of $\frac{1}{3}$ in the paper according to private communication with the author.
6. Y. Kubota *et al.*, CLEO Collaboration, Nucl. Instrum. Meth. A 320 (1992) 66; D. Peterson et al., Nucl. Instrum. Meth. A 478 (2002) 142.
7. T. Coan, Nucl. Instrum. Meth. A 379 (1996) 448.
8. M. Artuso et al., CLEO Collaboration, Nucl. Instrum. Meth. A 502 (2003) 91.
9. E. Farhi, Phys. Rev. Lett. 39 (1977) 1587.
10. We have measured the "wrong-sign" decays, $\tau^- \to \pi^-K^+\pi^-\pi^0\nu_\tau$ and $K^-\pi^+K^-\pi^0\nu_\tau$, observing no excess of events, indicating a reliable estimate of the fake rate.

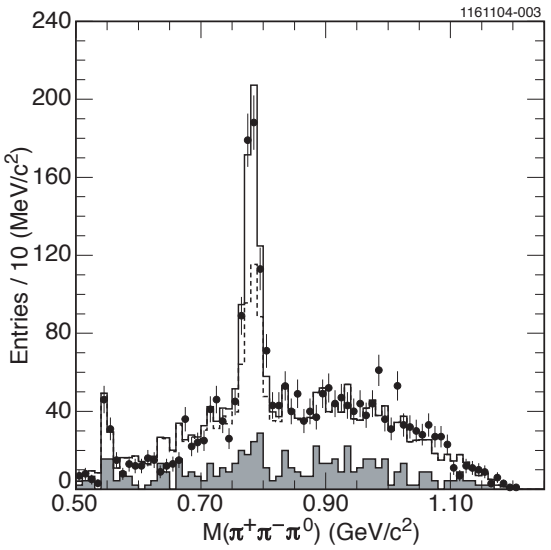

Figure 4. $\pi^+\pi^-\pi^0$ invariant mass spectrum in $\tau^- \to K^-\pi^+\pi^-\pi^0\nu_\tau$ events. The histogram shows the expectation using an equal mixture of $K_1(1400)$ and $K_1(1270)$, including τ-migration Monte Carlo events (dashed) and hadronic background (shaded). Error bars are statistical only.

11. The spin-dependent Breit-Wigner shape used is of the form $f(s) \propto \frac{\sqrt{s}m\Gamma}{(s-m^2)^2+m^2\Gamma^2}$.
12. S. Jadach and Z. Was, Comput. Phys. Commun. 36 (1985) 191; 64 (1991) 267; S. Jadach, J. H. Kuhn, and Z. Was, ibid. 64 (1991) 275.
13. R. Brun et al., CERN Report No. CERN-DD/EE/84-1, 1987 (unpublished).
14. The estimation of the significance includes the errors in the τ-migration and hadronic backgrounds only, as other systematic errors do not directly affect the significance of the signal.
15. G.J. Feldman and R.D. Cousins, Phys. Rev. D 57 (1998) 3873.
16. J.E. Bartelt et al., CLEO Collaboration, Phys. Rev. Lett. 76 (1996) 4119.
17. D. Buskulic et al., ALEPH Collaboration, Z. Phys. C 74 (1997) 263.
18. S. Eidelman et al., Particle Data Group, Phys. Lett. B 592 (2004) 1.
19. The absolute prediction for $\mathcal{B}(\tau^- \to K^-\rho^0\nu_\tau)$ is significantly lower than the experimental result.
20. The ratio $\mathcal{B}(\tau^- \to K^-\omega\nu_\tau)/\mathcal{B}(\tau^- \to K^-\pi^+\pi^-\pi^0\nu_\tau$, ex. $K^0) = (0.554 \pm 0.056 \pm 0.063)$ is a bit higher than but consistent with the ratio $\mathcal{B}(\tau^- \to h^-\omega\nu_\tau)/\mathcal{B}(\tau^- \to h^-h^+h^-\pi^0\nu_\tau$, ex. $K^0) = (0.446 \pm 0.015)$ [18], suggesting a similar hadronization pattern in $\tau^- \to K^-\pi^+\pi^-\pi^0\nu_\tau$ and $\tau^- \to \pi^-\pi^+\pi^-\pi^0\nu_\tau$ decays.